

Entanglement and Entropy Engineering of Atomic Two-Qubit States

S. G. Clark and A. S. Parkins

Department of Physics, University of Auckland, Private Bag 92019, Auckland, New Zealand
(Received 26 March 2002; published 31 January 2003)

We propose a scheme employing quantum-reservoir engineering to controllably entangle the internal states of two atoms trapped in a high-finesse optical cavity. Using laser and cavity fields to drive two separate Raman transitions between stable atomic ground states, a system is realized corresponding to a pair of two-state atoms coupled collectively to a squeezed reservoir. Phase-sensitive reservoir correlations lead to entanglement between the atoms, and, via local unitary transformations and adjustment of the degree and purity of squeezing, one can prepare entangled mixed states with any allowed combination of linear entropy and entanglement of formation.

DOI: 10.1103/PhysRevLett.90.047905

PACS numbers: 03.65.Ud, 03.67.-a, 42.50.-p

The properties of entangled mixed states and schemes for their controlled preparation are presently under vigorous investigation, primarily because of their relevance to understanding the role of purity and entanglement in quantum computation and quantum communication [1]. The purity and degree of entanglement of two-qubit states can be quantified, respectively, by the linear entropy and either the entanglement of formation or the concurrence [2,3]. Here, we propose a scheme using interactions in cavity quantum electrodynamics (CQED) to prepare states of two atomic qubits with *any* allowed combination of linear entropy and concurrence.

Our scheme uses the technique of quantum-reservoir engineering [4] in a CQED setting to couple a pair of two-state atoms collectively to an effective squeezed reservoir. The phase-sensitive quantum correlations of the reservoir are transferred to the atoms to produce entangled atomic states [5,6]. The purity and entanglement of these states can be controlled through the excitation time, through properties of the effective squeezing, and through the relative strengths of amplitude and phase coupling to the reservoir. We are thus able to scan the entire allowed region of the linear entropy-concurrence (LEC) plane, including the region between the Werner states [7] and the recently characterized maximally entangled mixed states (MEMS) [2]. Other CQED schemes for entangling a pair of atoms have been proposed and even implemented (see, e.g., [8–10]), but these focus mainly on preparing maximally entangled pure states.

In our proposal, two atoms are assumed to be tightly confined inside a high-finesse optical cavity and separated by a large enough distance that they feel no direct dipole-dipole interaction. Note, however, that the schemes we will describe enable us to access *most* of the allowed region of the LEC plane *without* the need to individually address each atom. The cavity has a field decay rate κ and a frequency ω , and may, if desired, be driven with broadband thermal light characterized by a mean photon number \bar{n} [11]. Two stable ground states ($|0\rangle$, $|1\rangle$) of each atom constitute the qubit states (Fig. 1).

The cavity field and two auxiliary laser fields drive two separate resonant Raman transitions between these states. In particular, transitions $|1\rangle \leftrightarrow |r\rangle$ and $|0\rangle \leftrightarrow |s\rangle$ are driven by detuned laser fields with (real) Rabi frequencies Ω_r and Ω_s and relative phase φ , while the transitions $|0\rangle \leftrightarrow |r\rangle$ and $|1\rangle \leftrightarrow |s\rangle$ are strongly coupled to the cavity mode, with coupling strengths g_r and g_s (assumed the same for both atoms). Detunings of the fields from the excited states $|r\rangle$ and $|s\rangle$ are Δ_r and Δ_s . A fifth state $|t\rangle$ is virtually excited from $|0\rangle$ by another strongly detuned laser field, adding an additional ac-Stark shift to the state $|0\rangle$.

The master equation for the total system density operator is (taking $\hbar = 1$)

$$\dot{\rho}_T = -i[H, \rho_T] + \mathcal{L}_{\text{cav}}\rho_T + \mathcal{L}_{\text{spon}}\rho_T, \quad (1)$$

where $H = H_{\text{cav}} + H_{\text{at}} + H_{\text{int}}$, with $H_{\text{cav}} = \omega a^\dagger a$,

$$H_{\text{at}} = \sum_{i=1,2} \{ \omega_r |r_i\rangle\langle r_i| + \omega_s |s_i\rangle\langle s_i| + \omega_t |t_i\rangle\langle t_i| + \delta |1_i\rangle\langle 1_i| + [(\Omega_r/2)e^{-i\omega_r t} |r_i\rangle\langle 1_i| + \text{H.c.}] \\ + [(\Omega_s/2)e^{-i[\omega_s t + \varphi]} |s_i\rangle\langle 0_i| + \text{H.c.}] + [(\Omega_t/2)e^{-i\omega_t t} |t_i\rangle\langle 0_i| + \text{H.c.}] \},$$

$$H_{\text{int}} = \sum_{i=1,2} (g_r |r_i\rangle\langle 0_i| a + g_s |s_i\rangle\langle 1_i| a + \text{H.c.}), \quad (2)$$

(H.c. denotes Hermitian conjugate) and

$$\mathcal{L}_{\text{cav}}\rho_T = \kappa(1 + \bar{n})(2a\rho_T a^\dagger - a^\dagger a\rho_T - \rho_T a^\dagger a) + \kappa\bar{n}(2a^\dagger\rho_T a - a a^\dagger\rho_T - \rho_T a a^\dagger). \quad (3)$$

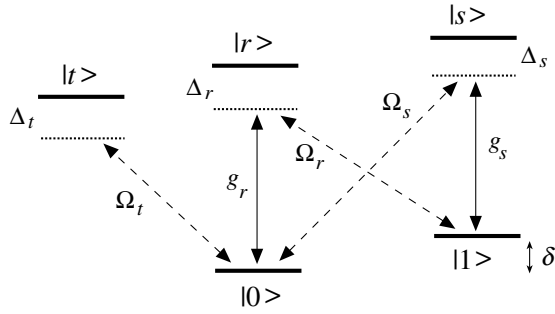


FIG. 1. Level scheme for each atom. The excited states have energies $\hbar\omega_j$ ($j = r, s, t$). Such an atomic configuration could be realized, e.g., with alkali atoms, where $|0\rangle$ and $|1\rangle$ are different ground-state hyperfine sublevels. Note also that $|r\rangle$ and $|s\rangle$ can be the same level, provided the two Raman channels remain distinct from each other (which would require $\delta \neq 0$).

Here, a is the cavity mode annihilation operator, ω_{Lj} ($j \in \{r, s, t\}$) denote the laser frequencies, and the term $\mathcal{L}_{\text{spont}}\rho_T$ describes atomic spontaneous emission.

$$\begin{aligned} \dot{\rho} = & (2\beta^2/\kappa)(N+1)(2S\rho S^\dagger - S^\dagger S\rho - \rho S^\dagger S) + (2\beta^2/\kappa)N(2S^\dagger \rho S - SS^\dagger \rho - \rho SS^\dagger) \\ & - (2\beta^2/\kappa)M(2S^\dagger \rho S^\dagger - S^\dagger S^\dagger \rho - \rho S^\dagger S^\dagger) - (2\beta^2/\kappa)M^*(2S\rho S - SS\rho - \rho SS) \\ & + (\eta^2/2\kappa)\bar{n}(\bar{n}+1)(2P\rho P^\dagger - P^\dagger P\rho - \rho P^\dagger P). \end{aligned} \quad (4)$$

Here, $\beta^2 = \beta_r^2 - \beta_s^2$, $\eta^2 = (\eta_r - \eta_s)^2$, and

$$N = \frac{(\bar{n}+1)\beta_s^2 + \bar{n}\beta_r^2}{\beta^2}, \quad M = \frac{-(2\bar{n}+1)\beta_r\beta_s e^{i\varphi}}{\beta^2},$$

while $S = (\sigma_1^- + \sigma_2^-)/\sqrt{2}$ and $P = \sigma_1^- \sigma_1^+ + \sigma_2^- \sigma_2^+$ are collective atomic operators, with $\sigma_i^- = |0_i\rangle\langle 1_i|$.

The derivation of (4) also requires that the phase of the effective two-level system remains constant with respect to the laser phase difference φ . That is, the effective atomic system and squeezed reservoir must be “resonant” with each other, which requires that

$$\frac{\Omega_s^2}{4\Delta_s} - \frac{\Omega_r^2}{4\Delta_r} + \frac{\Omega_t^2}{4\Delta_t} + \frac{g_r^2}{\Delta_r} \bar{n} - \frac{g_s^2}{\Delta_s} \bar{n} = 0. \quad (5)$$

It is to satisfy this condition while retaining flexibility in our choices of $\Omega_{r,s}$ and $\Delta_{r,s}$ that we use the additional transition $|0\rangle \leftrightarrow |t\rangle$. The level shift $\Omega_t^2/(4\Delta_t)$ provides an extra degree of freedom with which to satisfy (5).

In (4), the β^2 terms describe the collective (amplitude) coupling of our effective two-level atoms to an effective squeezed reservoir, with the degree and purity of squeezing characterized by the parameters $\{N, M\}$ [5,6]; i.e., the effective squeezed quadrature variance is proportional to $(N - |M| + 1/2)$ and ideal squeezing ($\bar{n} = 0$) corresponds to $|M|^2 = N(N+1)$. The last line of (4) describes phase damping of the atomic qubits caused by coherent scattering of off-resonant thermal intracavity photons.

A feature of the present system is that the strengths of the amplitude and phase damping terms are indepen-

To isolate the essential dynamics, we assume large detunings of the light fields from the excited atomic states (i.e., $|\Delta_j| \gg \Omega_j, g_r, g_s, \kappa, \gamma_j$, where γ_j is the linewidth of state $|j\rangle$), so that atomic spontaneous emission is negligible and the excited states can be adiabatically eliminated from the problem. This leads to a reduced master equation for a pair of effective two-level atoms (involving states $|0\rangle$ and $|1\rangle$) coupled to the cavity mode. This reduced system is characterized by the parameters

$$\beta_k = g_k \Omega_k / (2\Delta_k), \quad \eta_k = g_k^2 / \Delta_k, \quad k \in \{r, s\},$$

where β_r and β_s are the two (Raman) coupling strengths, and η_r and η_s are the ac-Stark shifts per cavity photon induced in $|0\rangle$ and $|1\rangle$, respectively.

To further reduce the model, we assume the “bad-cavity” limit, $\kappa \gg |\beta_{r,s}|, |\eta_{r,s}|$. This enables us to adiabatically eliminate the cavity mode, which yields a master equation for the atomic density matrix in the form

dently adjustable, so that, for example, one can be made to dominate the other [remembering that (5) must remain satisfied]. Also, by switching off all sources of light (i.e., setting $\beta_r = \beta_s = 0$ and $\bar{n} = 0$), the state of the two-atom system can in principle be “frozen” at any instant.

To begin our analysis of (4), we note first that associated with the collective coupling of the atoms to the reservoir are certain decoherence-free states, which decouple completely from the dynamics [10]. In particular, defining $|\phi^\pm\rangle = (|00\rangle \pm |11\rangle)/\sqrt{2}$ and $|\psi^\pm\rangle = (|01\rangle \pm |10\rangle)/\sqrt{2}$, one finds that $|\psi^-\rangle$ decouples for all parameter choices, while $|\psi^+\rangle$ decouples if $N = M = 0$.

As a first example, we consider the case in which phase damping can be neglected (i.e., $\bar{n} = 0$ or $\eta^2 \ll \beta^2$). The steady state density matrix ρ_{ss} is then, assuming an initial state that has no projection onto $|\psi^-\rangle$, given by

$$\rho_{\text{ss}} = \begin{pmatrix} \rho_{11} & 0 & 0 & \rho_{14} \\ 0 & \rho_{22} & \rho_{23} & 0 \\ 0 & \rho_{32} & \rho_{33} & 0 \\ \rho_{41} & 0 & 0 & \rho_{44} \end{pmatrix}, \quad (6)$$

specified in the basis $\{|11\rangle, |10\rangle, |01\rangle, |00\rangle\}$, with

$$\rho_{11} = \frac{|M|^2(1-2N) + N^2(1+2N)}{(1+2N)L},$$

$$\rho_{22} = \rho_{33} = \rho_{23} = \frac{1}{6} - \frac{1}{6L}, \quad \rho_{14} = \frac{M}{(1+2N)L},$$

where $L = 1 + 3N(1+N) - 3|M|^2$.

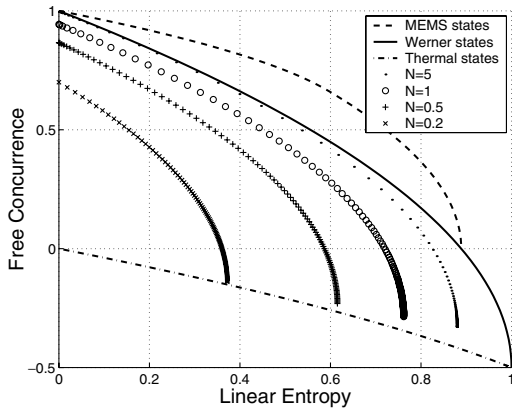


FIG. 2. Steady state values of $C_{\text{free}}(\rho)$ and $S_L(\rho)$ for selected values of N and $0 \leq |M|^2 \leq N(N+1)$, for initial state $|00\rangle$. For $|M|^2 < N(N+1)$ (nonideal squeezing), we require $\bar{n} \neq 0$.

Examples of the steady state and time evolution to the steady state are shown in Figs. 2 and 3, respectively, plotted as points in the LEC plane. We plot a minor variation of the true definition of the concurrence and call it the *free concurrence* $C_{\text{free}} = (\lambda_1 - \lambda_2 - \lambda_3 - \lambda_4)$, where λ_{1-4} are the square roots of the eigenvalues, in decreasing order, of $\rho\tilde{\rho}$, where $\tilde{\rho} = (\sigma_y \otimes \sigma_y)\rho^*(\sigma_y \otimes \sigma_y)$, with $\sigma_y = -i(\sigma^+ - \sigma^-)$. The use of the free concurrence enables separable states ($C_{\text{free}} \leq 0$) to be more readily distinguished. The linear entropy is given by $S_L(\rho) = (4/3)[1 - \text{Tr}(\rho^2)]$. On each graph, we also plot lines corresponding to the Werner states, $\rho_W = \xi|\phi^+\rangle\langle\phi^+| + (1/4)(1 - \xi)\mathbb{1}_4$ ($0 \leq \xi \leq 1$), the MEMS of [2], which have the maximum amount of entanglement for a given linear entropy, and thermal states $\rho_{\text{th}} = [\zeta|0\rangle\langle 0| + (1 - \zeta)|1\rangle\langle 1|]^{\otimes 2}$ ($0 \leq \zeta \leq 1$).

For ideal squeezing $\rho_{\text{ss}} = |\Psi_s\rangle\langle\Psi_s|$, a *pure state* [5] given by

$$|\Psi_s\rangle = \sqrt{\frac{N+1}{1+2N}}|00\rangle - e^{i\varphi}\sqrt{\frac{N}{1+2N}}|11\rangle, \quad (7)$$

which approaches the Bell states $|\phi^\pm\rangle$ in the limit of large squeezing (i.e., large N , and $\varphi = \pi$ or 0). Nonideal squeezing (Fig. 2) generates steady states that can lie essentially anywhere below the Werner line. Note that for large N the steady states closely approximate mixtures of $|\phi^+\rangle\langle\phi^+|$ ($\varphi = \pi$) and $\rho' = \text{diag}\{1/3, 1/6, 1/6, 1/3\}$.

Time evolution with ideal squeezing from initial states with zero projection onto $|\psi^-\rangle$ can also sweep out the region beneath the Werner line (Fig. 3). When the initial state *does* have a projection onto $|\psi^-\rangle$ (e.g., $|01\rangle$), an interesting range of points on the plane can also be accessed, including an area above the Werner line and the region along the boundary at $C_{\text{free}} = 0$ between separable and entangled (including the maximally mixed entangled state at the intersection of the Werner and MEMS lines).

States above the Werner line can also be generated by initially preparing the separable pure superposition state,

$$|\Psi(0)\rangle = \{\cos(\theta/2)\mathbb{1}_2 + i\sin(\theta/2)\sigma_y\}^{\otimes 2}|00\rangle, \quad (8)$$

with $0 < \theta \leq \pi/2$, and then applying the effective reservoir interaction with strong, ideal squeezing. In this case, the time evolution follows paths as shown in Fig. 4.

There is a small region of high entropy above the Werner line that cannot be reached by this method. However, this region can be accessed by switching off the squeezed reservoir interaction ($\beta_{r,s} = 0$) and employing phase decay ($\eta, \bar{n} \neq 0$) from initial states prepared on the $\theta = \pi/2$ curve of Fig. 4 and to which the local unitary transformation $U = (1/2)\{\sigma_x + \sigma_z\} \otimes \{\mathbb{1}_2 - i\sigma_y\}$ (requiring single-atom addressing with appropriate laser Raman pulses) has first been applied. This is also illustrated in Fig. 4. This may not be the optimum way to

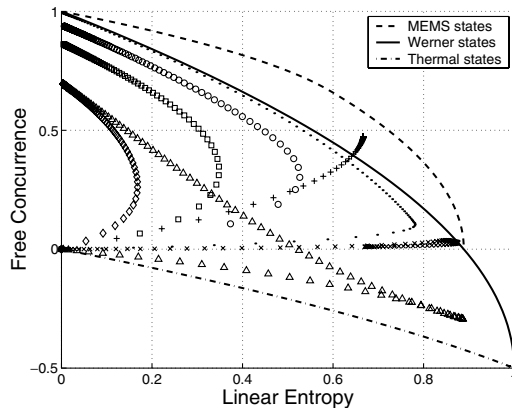


FIG. 3. Evolution of $C_{\text{free}}(\rho)$ and $S_L(\rho)$ to the steady state with ideal squeezing [$|M|^2 = N(N+1)$] for the following initial states and values of N : $\{|00\rangle, N = 0.2\}$ (\diamond), $\{|00\rangle, N = 0.5\}$ (\square), $\{|00\rangle, N = 1\}$ (\circ), $\{|00\rangle, N = 5\}$ (\bullet), $\{|11\rangle, N = 0.2\}$ (\triangle), $\{|01\rangle, N = 2\}$ (\times), and $\{|01\rangle, N = 0.01\}$ ($+$). Note that the points on each curve are not equally spaced in time.

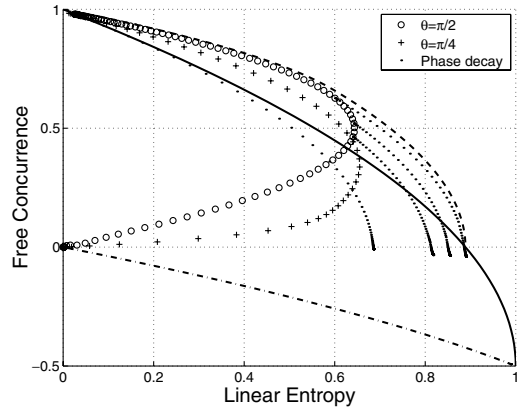


FIG. 4. Evolution of $C_{\text{free}}(\rho)$ and $S_L(\rho)$ for initial states (8) with $\theta = \{\pi/4, \pi/2\}$, $N = 3.1$, and $\bar{n} = 0$. The dotted curves show evolution produced by phase decay turned on after application of the unitary transformation U to a selection of states from the $\theta = \pi/2$ curve. For this evolution, amplitude coupling is disabled, but $\eta \neq 0$ and $\bar{n} = 1$.

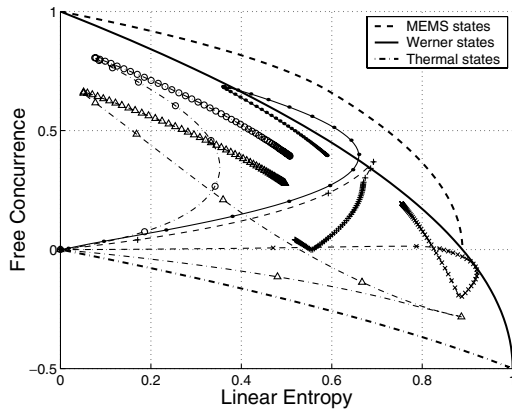


FIG. 5. Evolution of $C_{\text{free}}(\rho)$ and $S_L(\rho)$ with spontaneous emission effects for $(g_r, g_s, \kappa, \gamma_j, \Omega_s, \Delta_j)/2\pi = (110, 110, 14.2, 5.2, 100, 8000)$ MHz ($j = r, s, t$), $\Omega_t^2 = \Omega_r^2 - \Omega_s^2$, and $\bar{n} = 0$, with the following initial states and values of Ω_r : $\{|00\rangle, \Omega_r = 173 (N = 0.5)\}$ (\bullet), $\{|11\rangle, \Omega_r = 245 (N = 0.2)\}$ (Δ), $\{|01\rangle, \Omega_r = 110 (N = 5)\}$ (\times), and $\{|01\rangle, \Omega_r = 458 (N = 0.05)\}$ ($+$). Note that the points are not equally spaced in time.

access this region; it would be desirable to avoid the (experimentally difficult) need for single-atom addressing, but we have not yet found a simpler scheme.

Further analysis of (4) shows that the slowest dynamical rate is $(4\beta^2/\kappa)(2N - 2|M| + 1)$, which exhibits the inhibited decay associated with atomic damping by a squeezed reservoir [12]. Including atomic spontaneous emission (due to finite excited state populations) in the model reveals characteristic rates $\gamma_j(\Omega_j^2/2\Delta_j^2)$. Taking the rate for $j = r$ to be the maximum, and setting $\bar{n} = 0$, the condition that spontaneous emission be negligible during the state preparation reduces to $2g_r^2/(\gamma_r\kappa) \gg [1 - \sqrt{N/(N+1)}]^{-2}$. This is the condition of strong coupling CQED, made more stringent, however, due to the inhibited atomic decay rate. If we consider a recent CQED experiment for which $(g, \kappa, \gamma)/2\pi = (110, 14.2, 5.2)$ MHz [13], then for $N = 2$ the above inequality reads as $332 \gg 30$, indicating that sufficiently strong coupling is experimentally realistic for achieving high levels of effective squeezing. Furthermore, setting, e.g., $\Omega_r/\Delta_r = 0.02$ and using the above parameters, the characteristic state preparation time is $\lesssim 50 \mu\text{s}$, which is orders of magnitude less than single-atom trapping times in tightly confining optical dipole traps (see, e.g., [14,15]).

Figure 5 shows sample evolutions from a model in which excited atomic states have been adiabatically eliminated, but in which effects of spontaneous emission plus the cavity mode dynamics are included. Using the CQED parameters quoted above, we see that a large area of the LEC plane can be accessed. With the inclusion of spontaneous emission, decay into the (weakly coupled) state $|\psi^-\rangle$ can occur for states with no initial projection

onto $|\psi^-\rangle$. This limits the maximal attainable concurrence and leads also, for the cases with $\langle\psi^-|\rho(0)|\psi^-\rangle = 0$, to a very slow decay of $C_{\text{free}}(\rho)$ and increase in $S_L(\rho)$ after rapid initial evolution to the optimal value of $C_{\text{free}}(\rho)$. Note again though that the evolution can be frozen at any point by turning off all of the light fields. Higher cavity finesses improve the performance of the scheme and should be accessible experimentally [16].

Experimental values of $C_{\text{free}}(\rho)$ and $S_L(\rho)$ could be determined from a tomographic reconstruction of the two-qubit density matrix, following, e.g., the general procedure described in [17] (and used in [1]). In the present context, this would involve unitary rotations of the atomic states via coherent Raman transitions, followed by state-selective fluorescence detection [15].

In conclusion, we have proposed a scheme for engineering atomic two-qubit states with any allowed combination of linear entropy and concurrence. Such states will permit detailed experimental investigation of purity and entanglement in quantum information protocols.

We acknowledge helpful discussions with S. Rebić and W. J. Munro. This work was supported in part by the Marsden Fund of the Royal Society of New Zealand.

-
- [1] A. G. White, D. F. V. James, W. J. Munro, and P. G. Kwiat, *Phys. Rev. A* **65**, 012301 (2001).
 - [2] W. J. Munro, D. F. V. James, A. G. White, and P. G. Kwiat, *Phys. Rev. A* **64**, 030302 (2001).
 - [3] The concurrence C is monotonically related to the entanglement of formation $E_F(\rho)$; i.e., $E_F[\rho] = h((1 + \sqrt{1 - C^2})/2)$, where $h(x) = -x\log_2 x - (1-x)\log_2(1-x)$.
 - [4] N. Lütkenhaus, J. I. Cirac, and P. Zoller, *Phys. Rev. A* **57**, 548 (1998).
 - [5] G. M. Palma and P. L. Knight, *Phys. Rev. A* **39**, 1962 (1989).
 - [6] G. S. Agarwal and R. R. Puri, *Opt. Commun.* **69**, 267 (1989); *Phys. Rev. A* **41**, 3782 (1990).
 - [7] R. F. Werner, *Phys. Rev. A* **40**, 4277 (1989).
 - [8] E. Hagley *et al.*, *Phys. Rev. Lett.* **79**, 1 (1997).
 - [9] S. Osnaghi *et al.*, *Phys. Rev. Lett.* **87**, 037902 (2001).
 - [10] M. B. Plenio, S. F. Huelga, A. Beige, and P. L. Knight, *Phys. Rev. A* **59**, 2468 (1999).
 - [11] Such driving may be achieved, e.g., using a single output mode of a nondegenerate parametric oscillator operated below threshold, as in the experiment of Q. A. Turchette *et al.*, *Phys. Rev. A* **58**, 4056 (1998).
 - [12] C. W. Gardiner, *Phys. Rev. Lett.* **56**, 1917 (1986).
 - [13] C. J. Hood *et al.*, *Science* **287**, 1447 (2000).
 - [14] J. McKeever *et al.*, quant-ph/0211013.
 - [15] D. Frese *et al.*, *Phys. Rev. Lett.* **85**, 3777 (2000).
 - [16] H. J. Kimble (private communication).
 - [17] D. F. V. James, P. G. Kwiat, W. J. Munro, and A. G. White, *Phys. Rev. A* **64**, 052312 (2001).